Study of boron effects on the reaction of Co and Si 1x Ge x at various temperatures

H. J. Huang, K. M. Chen, C. Y. Chang, T. Y. Huang, T. C. Chang, L. P. Chen, and G. W. Huang

Citation: Journal of Vacuum Science & Technology A **18**, 1448 (2000); doi: 10.1116/1.582368
View online: http://dx.doi.org/10.1116/1.582368
View Table of Contents: http://scitation.aip.org/content/avs/journal/jvsta/18/4?ver=pdfcov
Published by the AVS: Science & Technology of Materials, Interfaces, and Processing

Study of boron effects on the reaction of Co and $Si_{1-x}Ge_x$ at various temperatures

H. J. Huang, K. M. Chen, C. Y. Chang,[a] and T. Y. Huang
Department of Electronic Engineering and Institute of Electronics, National Chiao-Tung University, Hsin-chu 30050, Republic of China

T. C. Chang, L. P. Chen, and G. W. Huang
National Nano Device Laboratory, Hsin-Chu, Republic of China

(Received 16 August 1999; accepted 10 January 2000)

The effects of boron on Co and $Si_{1-x}Ge_x$ interfacial reaction were studied. Undoped and *in situ* boron-doped strained $Si_{0.91}Ge_{0.09}$ and $Si_{0.86}Ge_{0.14}$ layers prepared at 550 °C by an ultrahigh vacuum chemical vapor deposition system were subjected to Co silicidation at various rapid thermal annealing (RTA) temperatures ranging from 500 to 1000 °C. The resulting films were characterized by a sheet resistance measurement, Auger electron spectroscopy, x-ray diffractometry (XRD), high resolution x-ray diffractometry, secondary ion mass spectroscopy, scanning electron microscopy, and transmission electron microscopy. Seen from XRD spectroscopy, a $Co(Si_{1-y}Ge_y)$ cubic structure was formed with RTAs ranging from 500 to 700 °C. For boron-doped samples, the CoGe fraction in $Co(Si_{1-y}Ge_y)$ was less than that in undoped samples, indicating that boron atoms retarded the incorporation of Ge into the $Co(Si_{1-y}Ge_y)$ ternary phase. It also led to a large Ge pileup at the interface between the Co-rich and silicidation regions. On the other hand, from the high resolution x-ray spectra, the presence of boron led to less relaxation of the strained $Si_{1-x}Ge_x$ lattice. It is the first time that small boron atoms inhibiting the relaxation of the $Si_{1-x}Ge_x$ layer during silicidation was observed. Furthermore, from the sheet resistance measurement, the formation of $CoSi_2$ was found to be slightly retarded in boron-doped samples, due probably to the decrease of Co or Si diffusivities as a result of boron accumulation at the Co/SiGe reaction interface. At temperatures above 800 °C, $CoSi_2$ formed and Ge segregated to the silicide boundaries and the upper reaction region was discovered. These phenomena caused by B dopants are explained in detail. © *2000 American Vacuum Society.* [S0734-2101(00)04604-2]

I. INTRODUCTION

Silicided strained-$Si_{1-x}Ge_x$ junctions have attracted lots of attention because of their potential applications to band-gap engineering by varying the Ge fraction in the $Si_{1-x}Ge_x$ layer. Recently advanced device structures based on the $Si_{1-x}Ge_x/Si$ heterojunction have been demonstrated.[1–4] In many device applications, it is necessary to make Schottky or ohmic contact with the epitaxial $Si_{1-x}Ge_x$ alloys. One example is the use of silicided strained-*p*-$Si_{1-x}Ge_x$ junctions in infrared detectors. With the addition of Ge in the strained $Si_{1-x}Ge_x$ layer, it is feasible to modulate and extend the cutoff wavelength.[5] Significant efforts have thus been made to understand the phase formations and properties of metal/$Si_{1-x}Ge_x$ reactions.[6–16]

Among the potential metal silicides, $CoSi_2$ is particularly attractive for its low resistivity, cubic crystal structure, relatively small lattice mismatch with Si, and its compatibility with the self-aligned silicide (salicide) scheme. At room temperature, the resistivity of $CoSi_2$ and its lattice constant mismatch with Si are 16 $\mu\Omega$ cm and 1.2%, respectively. Three cobalt silicide phases, i.e., Co_2Si, CoSi, and $CoSi_2$, form in sequence when a Co/Si bilayer structure is annealed.[17,18] The formation temperatures of CoSi and $CoSi_2$ are ~400 and 550 °C, respectively. In addition, Co_5Ge_7 and $CoGe_2$ phases are formed after annealing a Co/Ge bilayer structure at temperatures of about 300 and 600 °C, respectively.[12,19] In the past few years, the reaction of the Co/strained-$Si_{1-x}Ge_x/Si$ system has been studied extensively.[11,12,15,16] Compound formation after thermal treatment and the stability of the strained $Si_{1-x}Ge_x$ layer during silicide formation were investigated. For the ternary phase diagram of the Co–Si–Ge system, a miscible ternary compound, $Co(Si_{1-y}Ge_y)$ ($y < 0.67$), was found after low temperature furnace annealing (in the range from 400 to 700 °C), which is based on the cubic CoSi structure.[20] However, the crystal structures of $CoSi_2$ (i.e., the cubic CaF_2 structure) and $CoGe_2$ (i.e., the orthorhombic structure) are different, and the reaction between Co and Si is favored more than the Co–Ge one. As a result, only the $CoSi_2$ phase is observed at higher temperatures (~ 700 °C by furnace annealing). Concurrently, surface accumulation of Ge in the form of Ge-rich $Si_{1-z}Ge_z$ precipitates is observed.[14,21]

The strained SiGe layer is widely used as the base in heterojunction bipolar transistors and as the raised source/drain in advanced metal–oxide–semiconductor (MOS) transistors. For such applications, the $Si_{1-x}Ge_x$ layer is usually heavily doped. Dopants will redistribute in the reaction region or may even affect the metal/$Si_{1-x}Ge_x$ reaction during thermal processing. The effects of high dopant concentration on the Co silicidation process and the redistribution of dop-

[a]Electronic mail: u8511522@cc.nctu.edu.tw

ants during silicidation were studied.[22] Surface accumulation of boron redistributed from the Si consumption layer was observed. Furthermore, a comparison between B and Sb dopants in $Co/Si_{0.8}Ge_{0.2}$ during silicidation was reported recently.[23] While both dopants were found to accumulate at the surface, boron atoms were also found to be trapped at the interface between the Co-rich surface layer and the monosilicide region. In addition, a significant accumulation of Ge between the unreacted SiGe and the silicided region was observed on boron-doped $Si_{0.8}Ge_{0.2}$ samples, suggesting that B and Ge redistributions occur. However, a detailed explanation of boron impact on $Co/Si_{1-x}Ge_x$ compound formation and Ge redistribution due to lattice relaxation is, to the best of our knowledge, still has not been given.

In this article, we study the interfacial reaction of Co with the strained $Si_{1-x}Ge_x$ layer, especially the effects of boron dopants on compound formation and lattice relaxation during silicidation. The phase formation at various rapid thermal annealing (RTA) temperatures and the structural characteristics were also examined. This study will be helpful for future device applications in $Si_{1-x}Ge_x$ heterojunction bipolar transistors and advanced MOS transistors with a raised silicided $Si_{1-x}Ge_x$ source/drain.

II. EXPERIMENTS

Strained single-crystal $Si_{1-x}Ge_x$ thin films with $x=0.14$ and 0.09 were grown by an ultrahigh vacuum chemical vapor deposition (UHVCVD) system.[24] The UHVCVD system included a loading chamber, a water-cooled stainless-steel growth chamber, separate nozzles for process gases, and a computer-controlled gas switching box. The growth chamber was pumped with a 1000 l/s turbomolecular pump to a base pressure of 2×10^{-10} Torr. As the starting substrates 10–15 Ω cm, *n*-type (100) silicon wafers were used. The wafers were first subjected to a pre-clean process using a hydrogen passivation technique. Afterwards, the wafers were loaded into the loading chamber and pumped down to 10^{-6} Torr with minimal delay. The wafers were then immediately transferred into the growth chamber for epitaxial growth. During the transfer process, the heater temperature was kept at 200 °C. A base pressure of 10^{-9} Torr was routinely obtained within 1 min of the wafer transfer process. Then, the wafers were heated to the final deposition temperature of 550 °C at a ramp rate of ~150 °C/min. For growing undoped $Si_{1-x}Ge_x$, pure Si_2H_6 and GeH_4 were introduced into the growth chamber. For growing *in situ* boron-doped $Si_{1-x}Ge_x$, a 1% B_2H_6 gas diluted in H_2 was added. The resultant boron concentration in the *in situ* boron-doped SiGe samples was found to be 1×10^{19} cm^{-3}, while the unintentionally doped (i.e., undoped) samples have a low boron doping level of about 1×10^{15} cm^{-3}. The chamber pressure was maintained below 10^{-3} Torr during epitaxial growth by the turbomolecular pump. The grown $Si_{1-x}Ge_x$ epitaxial layer thickness was 100 nm for all samples used in this study.

The wafers with a grown $Si_{1-x}Ge_x$ layer were then cleaned by a standard RCA clean and dipped in HF:H_2O (1:50) for 30 s to remove the native oxide. After a rinse and a spin dry, the wafers were loaded into a sputter deposition chamber to deposit a 17 nm thick Co thin film. The Co film was deposited by ion beam sputtering with a base pressure of 5×10^{-9} Torr and the sputtering rate of Co film was 2 nm/s. Next, a 30 nm thick TiN capping layer was deposited on top of the Co film. The purpose of the TiN capping layer was to prevent oxidation of the metal film and also to improve the uniformity of the silicide formation.[25,26] The $Co/Si_{1-x}Ge_x$ reaction was performed in a RTA system equipped with high-intensity halogen tungsten lamps. The RTA treatment was carried out in nitrogen ambient for 30 s at different RTA temperatures. After the silicidation process, the TiN capping layer and the unreacted Co film were removed selectively by wet etching in a $4H_2SO_4$:$1H_2O_2$ (30%) solution for 5 min. The sheet resistance was measured by a conventional four-point probe measurement system while the structural and compositional properties of the reacted thin films were carefully examined by x-ray diffractometry (XRD), high resolution x-ray diffraction with high energy x-ray beams, Auger electron spectroscopy (AES), and secondary ion mass spectroscopy (SIMS). The high resolution asymmetric θ-2θ x-ray diffraction measurements consisted of a Huber Cu target source with a Si(111) crystal monochromator and a Ragaku scintillation NaI detector to detect the diffracted beams. The sample was mounted in air at the center of the five-circle diffractometer axes. SIMS measurements were performed in a Cameca IMS5*f* apparatus. To obtain better accuracy, boron and oxygen profiles were obtained using O_2^+ and Cs^+, respectively, as the primary ion beams. Finally, the morphologies of the surfaces and interfaces were analyzed using scanning electron microscopy (SEM) and cross-sectional transmission electron microscopy (XTEM).

III. RESULTS AND DISCUSSION

Figures 1 and 2 are the AES depth profiles with different rapid thermal annealing temperatures for undoped and boron-doped $Co/Si_{1-x}Ge_x/Si$ layers, respectively. For the samples that have undergone RTA at 500 °C for 30 s, both the undoped and the B-doped samples exhibit a uniform layer of Co, Si, and Ge on top of the $Si_{1-x}Ge_x/Si$ layer. From x-ray diffractometry, reaction of $Co/Si_{1-x}Ge_x$ at 500 °C results in the CoSi phase or the $Co(Si_{1-y}Ge_y)$ ternary phase, both of which will be discussed in more detail later. It should be noted that a Co_2Si phase could not be observed in our study because this compound can also be etched by the same etching recipe used to selectively remove the unreacted Co and TiN capping layers. From Figs. 1(a) and 2(a), it can be seen that, for B-doped samples, Ge is released from the monosilicide region and accumulates near the surface during preferential reaction of Si with Co. In addition, the relative atomic ratio of Ge to Si for the B-doped sample in the middle of the reacted layer was less than that of the undoped sample in the same reaction. This means that the Ge composition of the $Co(Si_{1-y}Ge_y)$ ternary phase in B-doped sample is smaller than that in the undoped sample.

After annealing at 700 °C for 30 s, the Co/Si sample was fully converted into the $CoSi_2$ phase, while mostly the CoSi

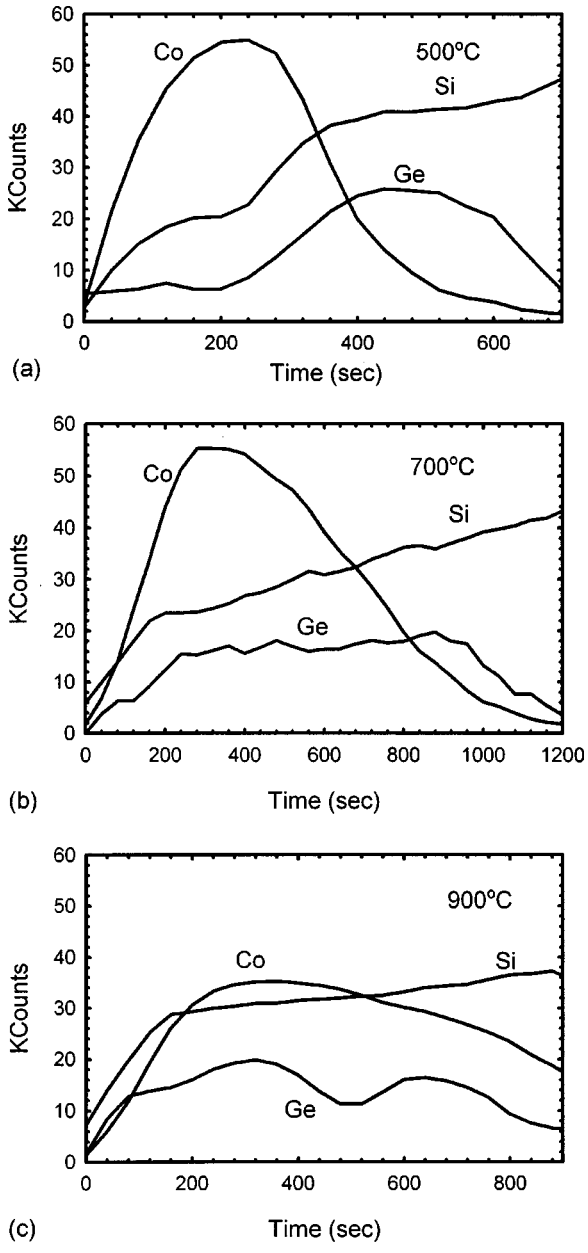

FIG. 1. AES depth profiles of the undoped Co (17 nm)/$Si_{0.86}Ge_{0.14}$ (100 nm) sample after (a) 500, (b) 700, and (c) 900 °C, 30 s annealing.

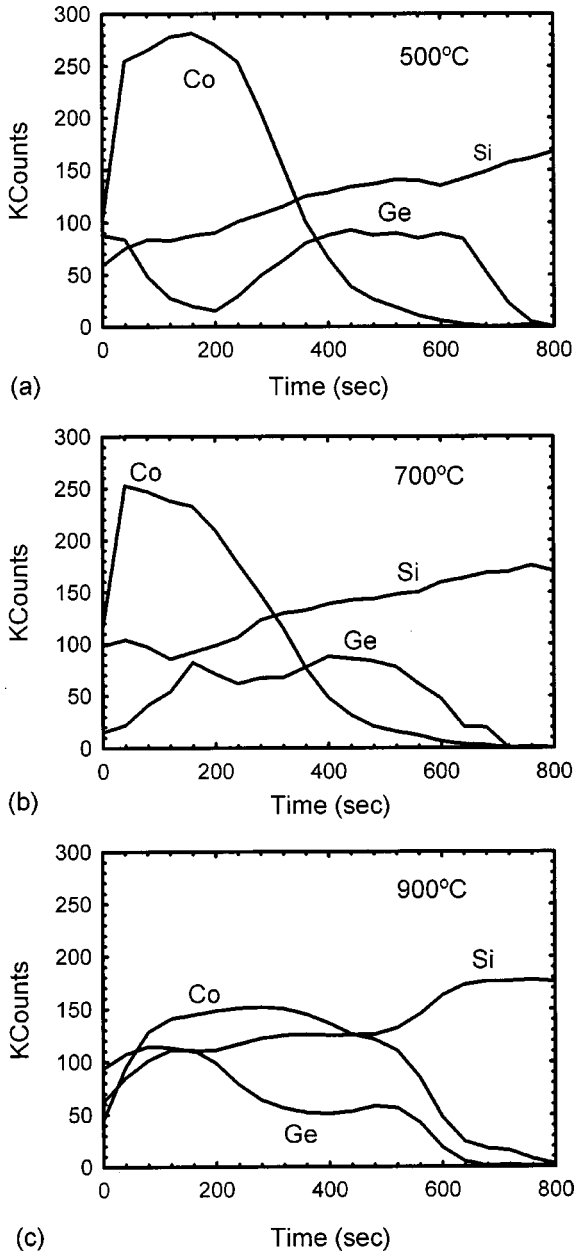

FIG. 2. AES depth profiles of the boron-doped Co (17 nm)/$Si_{0.86}Ge_{0.14}$ (100 nm) sample after (a) 500, (b) 700, and (c) 900 °C, 30 s annealing.

phase and a little $CoSi_2$ phase were discovered for all the $Si_{1-x}Ge_x$ base samples. For the B-doped sample, Ge accumulation was observed in the middle of the reacted Co/$Si_{1-x}Ge_x$ layer, while a Si pileup was observed near the surface.

With the 900 °C RTA, both the undoped and the B-doped samples showed an obvious Ge pileup at the upper region of the Co/$Si_{1-x}Ge_x$ reaction layer. This pileup was even more pronounced in the B-doped sample. In addition, the number of Co atoms near the surface decreased compared to samples with 700 °C RTA. Figures 1(c) and 2(c) also reveal that Co is well distributed over the entire $Si_{1-x}Ge_x$ layer at higher temperature. From AES data, it can be seen that the greater Ge loss in the unreacted B-doped $Si_{1-x}Ge_x$ layer, which had been reported recently,[23] was not observed in our experiments. In contrast, the Ge losses, Δx, from the underlying undoped $Si_{1-x}Ge_x$ sample is higher than that in the B-doped $Si_{1-x}Ge_x$ sample. As shown in Fig. 1, Δx for the undoped sample annealed 500 to 700 °C is 0.019 whereas Δx for the B-doped sample annealed 500 to 700 °C is 0.011.

Figure 3 demonstrates the dependence of sheet resistance on the RTA temperatures for undoped and B-doped Co/$Si_{1-x}Ge_x$ (100 nm) layers. Conventional Co/Si samples were also measured for a comparison. At 500 °C, the sheet resistance of the Co/Si sample is much higher than that of the Co/$Si_{1-x}Ge_x$ sample. This is probably because of the relative low resistivity of the CoGe phase formation. On the other

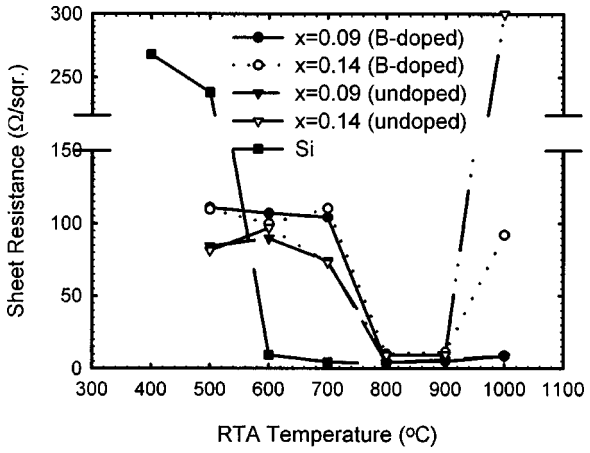

FIG. 3. Sheet resistance as a function of RTA temperature for Co (17 nm)/$Si_{1-x}Ge_x$ (100 nm) and Co (17 nm)/Si control samples.

hand, the sheet resistance of the reacted Co/$Si_{1-x}Ge_x$ films after 600 and 700 °C annealing is much higher than that of the Co/Si samples. This is believed to be due to the formation of a Ge-rich surface layer by Ge segregation and highly resistive CoSi growth. From the x-ray diffraction spectra, it is seen that the $CoSi_2$ phase has already formed for the Co/Si reaction at these intermediate temperatures (i.e., 600 and 700 °C). It is further seen from sheet resistance measurements that the sheet resistance begins to decrease for undoped samples with 700 °C annealing, but the sheet resistance for B-doped samples remains high. This indicates that the formation of $CoSi_2$ is retarded in boron-doped samples. This may be due to the decrease in Co or Si diffusion as a result of B and Ge accumulation at the Co/$Si_{1-x}Ge_x$ reaction interface. Moreover, the sheet resistance of all the samples is reduced to less than 10 Ω/□ after 800 and 900 °C annealing, indicating the conversion of CoSi phase to $CoSi_2$ phase. However, the sheet resistance of the $Si_{0.86}Ge_{0.14}$ sample increases dramatically again at 1000 °C, implying that the agglomeration phenomenon is more serious for the Co/$Si_{1-x}Ge_x$ sample with a higher Ge mole fraction.

The SIMS depth profiles for B-doped Co/$Si_{0.86}Ge_{0.14}$ samples are shown in Fig. 4 for samples with various annealing temperatures. For the sample with 500 °C RTA [Fig. 4(a)], surface accumulation of boron is found. Additionally, about $4\times10^{19}\,cm^{-3}$ of boron atoms has accumulated in the upper Co/$Si_{1-x}Ge_x$ reaction region for both samples with 700 [Fig. 4(b)] and 900 °C [Fig. 4(c)] RTA. This phenomenon is believed to be associated with Ge and Si out diffusion during the silicidation process.

The phase formation sequence during Co reaction with $Si_{0.86}Ge_{0.14}$ and the crystallographic orientation of silicide were monitored by symmetric x-ray diffraction in θ-2θ geometry. Figure 5 shows undoped Co/$Si_{0.86}Ge_{0.14}$ XRD spectra at various RTA temperatures. We can see that at 500 °C RTA, the predominant phase is Co($Si_{1-y}Ge_y$) in all samples, since the Co_2Si phase may have been removed during selective wet etching of the TiN/Co film. At 800 °C, disilicide phases can be identified. In addition, the (200) and (400)

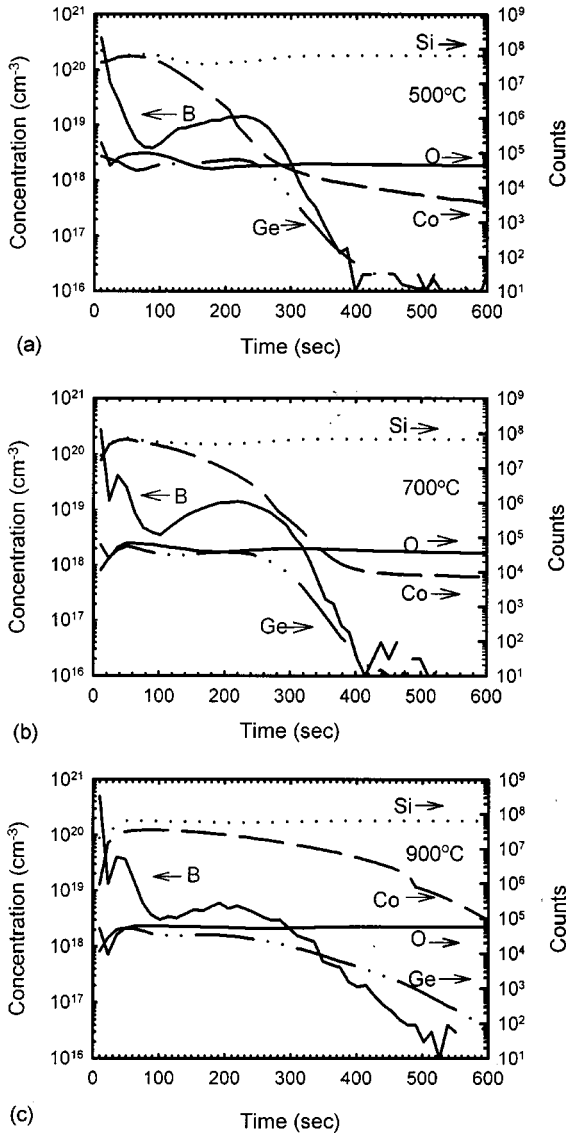

FIG. 4. SIMS depth profiles of the boron-doped Co (17 nm)/$Si_{0.86}Ge_{0.14}$ (100 nm) sample after (a) 500, (b) 700, and (c) 900 °C, 30 s annealing. The boron doping concentration is $1\times10^{19}\,cm^{-3}$.

orientations of the disilicide phases are very pronounced compared to other diffraction peaks in the XRD spectra. This indicates that the main crystal orientation of $CoSi_2$ (n00) is the same as that of the $Si_{1-x}Ge_x$ epitaxy. Finally, after annealing at 900 and 1000 °C, the orientation behavior becomes more obvious than that of the 800 °C sample. The (111) and (220) orientations of the $CoSi_2$ peaks could not be observed for all samples at these temperatures. No Co($Si_{1-x}Ge_x$)$_2$ is found after high temperature Co/$Si_{1-x}Ge_x$ reaction.

A ternary compound is not likely to form if the precursor Si–metal compound and Ge–metal compound are different in structure. Previous studies indicate that in the Co–Si–Ge system, there are two solid-solution regions.[20] In the CoSi phase, up to two thirds of the Si atoms may be replaced by the Ge atoms. Both CoSi and CoGe form cubic crystalline structures with similar lattice constants (i.e., 4.43 Å for CoSi and 4.637 Å for CoGe). This leads to the formation of

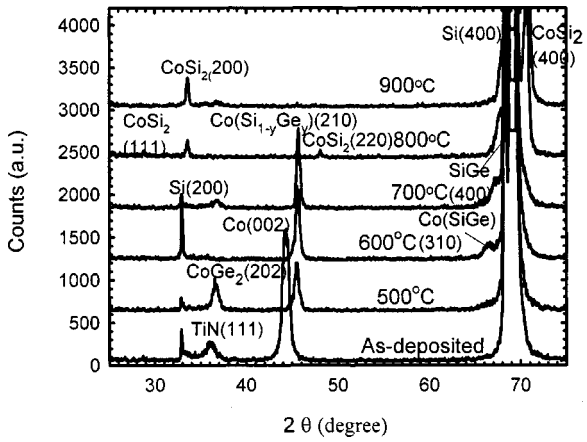

FIG. 5. XRD spectra of 17 nm Co deposited on the undoped 100 nm $Si_{0.86}Ge_{0.14}$ layer after annealing at different temperatures for 30 s.

$Co(Si_{1-y}Ge_y)$ ternary compounds, which can be calculated from the shifts of the CoSi peak position in the XRD spectra due to expansion of the CoSi lattice, shown in Fig. 6(a). The interplanar distance d of $Co(Si_{1-y}Ge_y)$, which is calculated by the relative amounts of CoSi and CoGe in the reacted film, can be expressed as follows:[11]

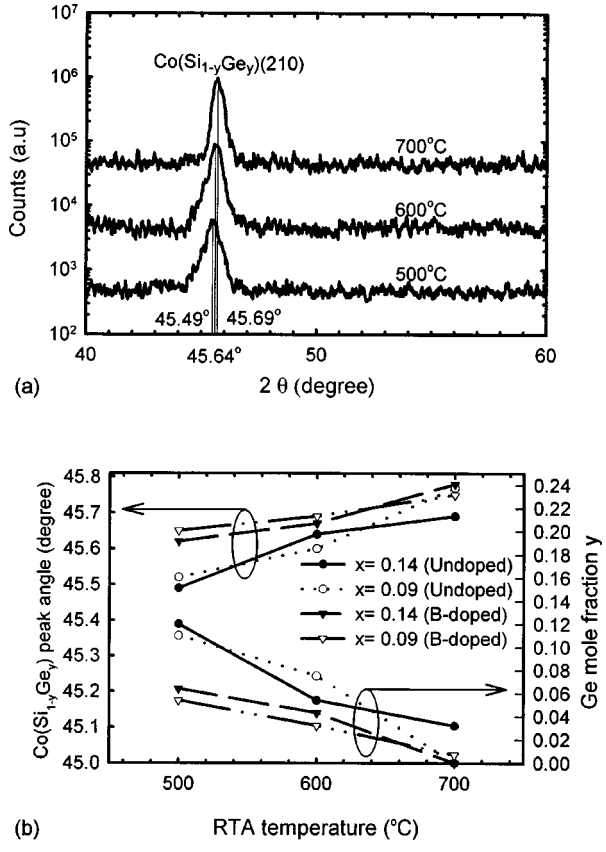

FIG. 6. (a) XRD spectra of the $Co(Si_{1-y}Ge_y)(310)$ phase for 17 nm Co deposited on the 100 nm undoped $Si_{0.86}Ge_{0.14}$ sample after different RTA conditions, and (b) the diffraction angle of the $Co(Si_{1-y}Ge_y)$ phase and the relative CoGe ratio y after rapid thermal anneals at different temperatures for different samples.

$$d_{Co(Si_{1-y}Ge_y)} = d_{CoSi}(1-y) + d_{CoGe}y. \quad (1)$$

The interplanar distance (d) is 1.981 and 2.074 Å for CoSi (210) and CoGe (210), respectively. After careful calculation of the $Co(Si_{1-y}Ge_y)$ (210) diffraction peaks, the ratio of CoGe to CoSi and CoGe (i.e., y) can be estimated, as shown in Fig. 6(b) for all samples. For B-doped samples with 500 °C annealing, the relative ratios of CoGe in $Co(Si_{1-y}Ge_y)$ compound y are 0.064 and 0.054 for the $Co/Si_{0.86}Ge_{0.14}$ and $Co/Si_{0.91}Ge_{0.09}$ samples, respectively. Moreover, these y values are nearly half the y values for undoped samples (i.e., $y \sim 0.12$ in the $Co/Si_{0.86}Ge_{0.14}$ sample and $y \sim 0.11$ in the $Co/Si_{0.91}Ge_{0.09}$ sample). These results imply that boron atoms may restrict the reaction between Co and Ge or enhance Ge segregation from the Co/SiGe reaction region. These results are also consistent with the AES depth profiles. As the RTA temperature increases, the y values for all samples decrease, meaning more severe Ge segregation in the Co/SiGe reaction region. It has been reported that the heat of formation of the equiatomic compound of CoSi (−7 kcal/g atom) is much lower than that for CoGe (−4 kcal/g atom). Thus, in the Co/SiGe reactions at 600 and 700 °C, Ge may be rejected in favor of the Co–Si reaction. Finally, only the $CoSi_2$ phase, not the $CoGe_2$, is formed at higher temperatures due to the low consumption of energy and small lattice mismatch.

Figures 7(a) and 7(b) demonstrate high-resolution XRD (400) asymmetric θ–2θ spectra of the undoped and B-doped $Co/Si_{0.86}Ge_{0.14}$ layers after annealing at different temperatures. The reaction of Co with $Si_{1-x}Ge_x$ layer could cause some changes in the quality of the $Si_{1-x}Ge_x$ structure. The underlying $Si_{1-x}Ge_x$ layer would be consumed gradually as the RTA temperature increases and then $Si_{1-x}Ge_x$ lattice relaxation would occur due to lattice mismatch with the upper Co silicide layer. Lattice relaxation of the underlying $Si_{1-x}Ge_x$ layer would cause a shift of the $Si_{1-x}Ge_x$(400) peak in the XRD spectra towards the Si (400) peak. Based on this shift, we can observe the degree of relaxation in the underlying SiGe region. After annealing at 700 °C, the shift angle for the undoped sample is 0.07° (i.e., from 68.21° to 68.28°), but the shift angle for the B-doped sample is only 0.04° (i.e., from 68.22° to 68.26°). A similar result was also obtained for the $Si_{0.91}Ge_{0.09}$ samples. Thus, we can conclude that for B-doped samples, lattice relaxation is inhibited. This also means that a small amount of boron ($\sim 1\times10^{19}\,cm^{-3}$) will decrease the mobility of misfit dislocations in the $Si_{1-x}Ge_x$ lattice, similar to that observed for C in the $Si_{1-x}Ge_x$ layer.[27] After a 900 °C anneal, the AES profiles indicate that the $Si_{1-x}Ge_x$ layer is totally consumed in all samples, so the $Si_{1-x}Ge_x$ peaks in the XRD spectra disappear. Moreover, from the sheet resistance data shown in Fig. 3, phase agglomeration in the $Si_{0.86}Ge_{0.14}$ sample occurred with a 1000 °C rapid thermal anneal. This is expected to worsen the surface roughness. The surface morphology seen in SEM micrographs for undoped $Co/Si_{0.86}Ge_{0.14}$ samples annealed at 900 and 1000 °C is shown in Figs. 8(a) and 8(b), respectively. It can be seen that the surface becomes much

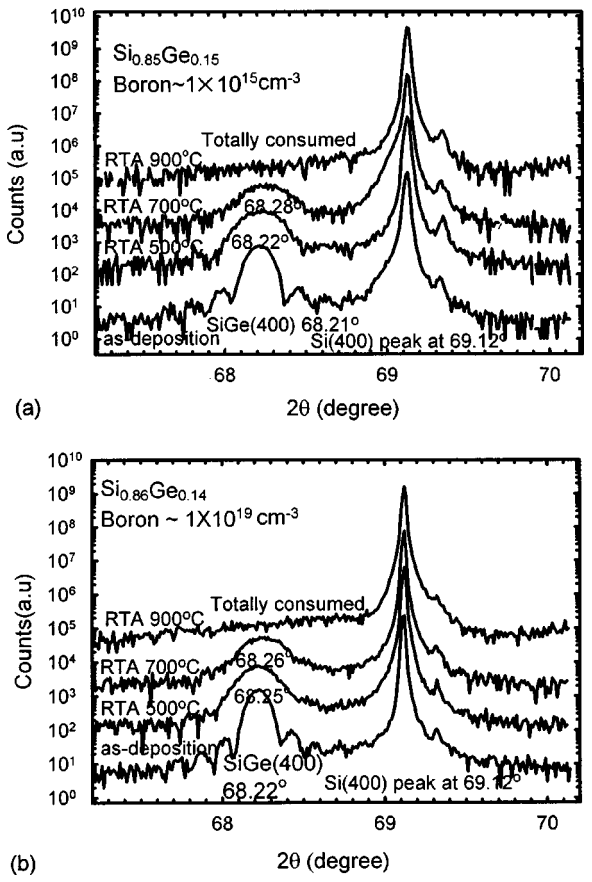

FIG. 7. High-resolution XRD spectra of Co (17 nm) deposited on (a) undoped and (b) B-doped $Si_{0.86}Ge_{0.14}$ layers after annealing at different temperatures for 30 s.

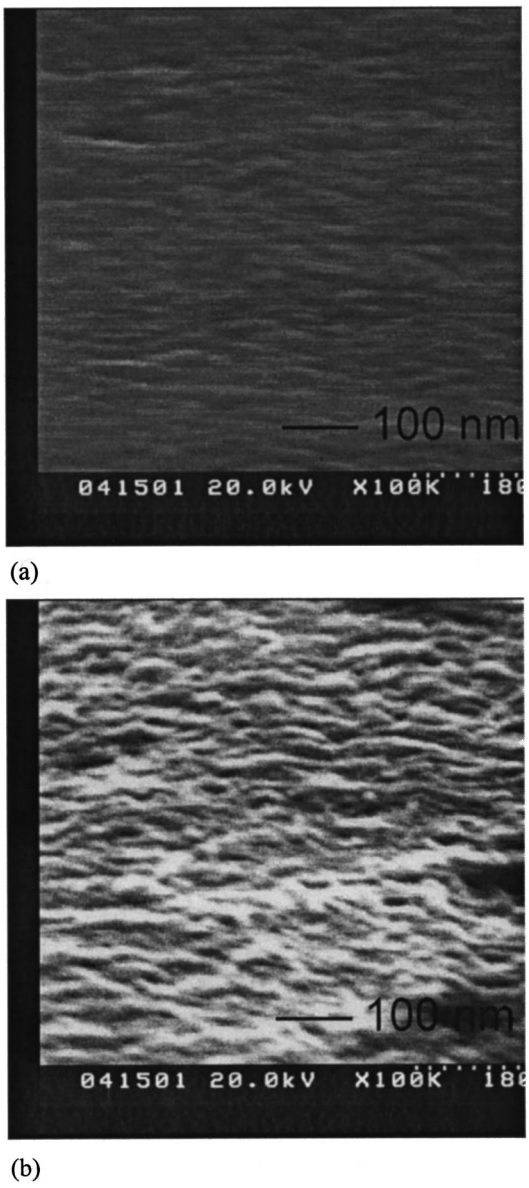

FIG. 8. SEM micrographs of the surface morphology of the undoped $Co/Si_{0.86}Ge_{0.14}$ sample annealed for 30 s at (a) 900 and (b) 1000 °C. After 1000 °C annealing, the surface is severely roughened, indicating the occurrence of agglomeration.

rougher by increasing the RTA temperature from 900 to 1000 °C.

Figure 9 is a TEM micrograph of the B-doped $Si_{0.86}Ge_{0.14}$ sample after 900 °C RTA. Based on XRD analysis, only the $CoSi_2$ phase is found at this temperature, and it is represented by the large grain in the TEM micrograph. The underlying $Si_{0.86}Ge_{0.14}$ layer is almost consumed and silicidation has extended into the Si region. Furthermore, we can see very clearly that there are some small decorations around the $CoSi_2$ grain boundaries. It has been reported that the decorations are Ge-rich $Si_{1-z}Ge_z(z>x)$ alloys.[23,28] $Si_{1-z}Ge_z$ precipitates segregate from the Co silicide region and become distributed mostly in the upper and bottom parts of the $Co/Si_{1-x}Ge_x$ reacted region. These results confirm the trends of the AES and SIMS profiles.

To elucidate the effects of the boron on silicide reaction and the lattice distortion at the underlying $Si_{1-x}Ge_x$ layer, we summarize below the important experimental results. At 500 °C, B accumulation is very near the surface. At 700 and 900 °C, boron atoms pile up at the upper $Co/Si_{1-x}Ge_x$ reaction layer, which is between the cobalt silicide and thin Co-rich surface layer. The same phenomenon can be observed from the interaction of Co with the B-doped Si sample at temperatures below 500 °C.[22] The reason for the B pileup may be the low solubility of boron in crystalline Co silicides ($\sim 5\times10^{19}\,cm^{-3}$). The boron atoms are pushed out of the $Co/Si_{1-x}Ge_x$ or Co/Si silicide region. For the case of conventional Co/Si, the boron atoms accumulate at the interface between CoSi and Co-rich layers after a low temperature anneal (500 °C). After higher temperature annealing (>500 °C), the Co-rich layer is consumed, so the boron atoms move to the surface region. For the $Co/Si_{1-x}Ge_x$ case, we assume that boron atoms segregate out of the monosilicide layer and are injected along the silicide grain boundaries or defects into the Ge-rich $Si_{1-z}Ge_z$ precipitates, where the solubility of boron is higher than it is in the silicide region. This assumption could explain the phenomenon that a B pileup still occurs at the upper silicide region in the $Co/Si_{1-x}Ge_x$ sample even after high temperature annealing

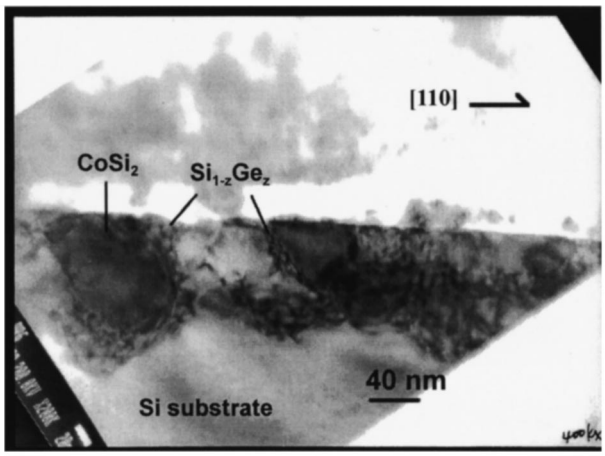

FIG. 9. Cross-sectional TEM micrograph of the B-doped $Si_{0.86}Ge_{0.14}$ sample after reaction with Co (17 nm) with a RTA at 900 °C for 30 s.

(700 and 900 °C). In addition, the reason why the boron pileup region is very close to the Ge accumulation region can also be explained. According to the diffraction angle of the $Co(Si_{1-y}Ge_y)$ (210) phase, the CoGe fraction of the sum of CoSi and CoGe, *y*, in the B-doped sample is indeed smaller than that in the undoped sample. This phenomenon may be explained by the fact that boron atoms tend to accumulate with Ge atoms. In other words, B atoms may grab Ge atoms to form B-doped $Si_{1-z}Ge_z$ clusters as the Si and Ge atoms diffuse toward the Co film. This is consistent with the results of the AES profiles that more Ge atoms tend to accumulate at the upper $Co/Si_{1-x}Ge_x$ reaction region in B-doped samples.

The other interesting effect is the reduced mobility of misfit dislocation for lattice distortion in the underlying B-doped $Si_{1-x}Ge_x$ layer by B atoms. Relaxation is accompanied by the formation and extension of dislocations along which the Ge and Si atoms could outdiffuse. Recently it was reported that a small-sized atom such as C could decrease the occurrence of misfit dislocation in the $Si_{1-x}Ge_x$ layer, and therefore inhibit lattice relaxation.[27] From our high resolution XRD spectra, the lattice relaxation is indeed retarded by B atoms, similar to the effect of C atoms in the $Si_{1-x}Ge_x$ layer.

IV. CONCLUSION

In this article, a detailed comparison of the Co reaction with undoped and *in situ* boron-doped strained $Si_{0.86}Ge_{0.14}$ and $Si_{0.91}Ge_{0.09}$ layers was made. Due to the low solubility of boron in the silicide film, boron atoms were found to segregate out of the silicide layer and were injected into the Ge-rich $Si_{1-z}Ge_z$ precipitates at the upper silicide region. In addition, more Ge atoms accumulated in the same region than the undoped sample. This means that boron pileup may cause the Ge-rich $Si_{1-z}Ge_z$ precipitates to accumulate in the upper silicide region. In addition, Ge segregation to the upper silicide region and to the monosilicide (and disilicide) boundaries was also observed from AES and TEM analyses. Furthermore, with more Ge segregation from monosilicide, a smaller fraction, *y*, of CoGe was incorporated into the $Co(Si_{1-y}Ge_y)$ ternary phase, as seen by the XRD spectra of the $Co(Si_{1-y}Ge_y)(210)$ phase. Finally, we discovered for the first time that the presence of boron atoms, similar to that of carbon ones, inhibited lattice relaxation of the underlying $Si_{1-x}Ge_x$ layer. This inhibition of lattice relaxation was probably because small atoms decrease the misfit dislocation mobility of the underlying $Si_{1-x}Ge_x$ layer.

ACKNOWLEDGMENTS

The authors would like to thank Dr. F. M. Pan, Dr. W. F. Wu, and Dr. H. C. Lin for experimental assistance. This work was supported in part by the National Science Council of the Republic of China (No. NSC88-2215-E009-048).

[1]X. Xiao, C. Sturm, S. R. Parihar, S. A. Lyon, D. Meyerhofer, S. Palfery, and F. V. Shallcross, IEEE Electron Device Lett. **EDL-14**, 199 (1993).
[2]G. L. Patton, J. H. Comfort, B. S. Meyerson, E. F. Crabbe, B. De Fresart, J. M. C. Stork, J. Y. C. Sun, D. L. Harame, and J. M. Burgatz, IEEE Electron Device Lett. **EDL-11**, 171 (1990).
[3]J. M. Stork, E. J. Prinz, and C. W. Magee, IEEE Electron Device Lett. **EDL-12**, 303 (1991).
[4]P. M. Garone, V. Venkataraman, and J. C. Sturm, Tech. Dig. Int. Electron Devices Meet. 90 (1990).
[5]H. Kanaya, F. Hasegawa, E. Yamaka, T. Moriyama, and M. Nakajima, Jpn. J. Appl. Phys., Part 1 **28**, 544 (1989).
[6]Q. Z. Hong and J. W. Mayer, J. Appl. Phys. **66**, 611 (1989).
[7]H. K. Liou, X. Wu, and U. Gennser, Appl. Phys. Lett. **60**, 577 (1992).
[8]R. D. Thompson, K. N. Tu, J. Angillelo, S. Delage, and S. S. Iyer, J. Electrochem. Soc. **135**, 3161 (1988).
[9]O. Thomas, F. M. D'Heurle, S. Delage, and G. Scilla, Appl. Surf. Sci. **38**, 27 (1989).
[10]O. Thomas, F. M. D'Heurle, and S. Delage, J. Mater. Res. **5**, 1453 (1990).
[11]W.-J. Qi, B.-Z. Li, W.-N. Huang, and Z.-Q. Gu, J. Appl. Phys. **77**, 1086 (1995).
[12]Z. Wang, Y. L. Chen, H. Ying, R. J. Nemanich, and D. E. Sayers, Mater. Res. Soc. Symp. Proc. **320**, 397 (1994).
[13]A. Buxbaum, M. Eizenberg, A. Raizman, and F. Schäffler, Appl. Phys. Lett. **59**, 665 (1991).
[14]M. C. Ridgway, R. G. Elliman, N. Hauser, J.-M. Baribeau, and T. E. Jackman, Mater. Res. Soc. Symp. Proc. **260**, 857 (1992).
[15]F. Lin, G. Sarcona, M. K. Hatalis, A. F. Cserhati, E. Austin, and D. W. Greve, Thin Solid Films **250**, 20 (1994).
[16]M. Glück, A. Schuppen, M. Rösler, W. Heinrich, J. Hersener, U. König, O. Yam, C. Cytermann, and M. Eizenberg, Thin Solid Films **270**, 549 (1995).
[17]A. Appelbaum, R. V. Knoell, and S. P. Murarka, J. Appl. Phys. **57**, 1880 (1985).
[18]G. Ottaviani, K. N. Tu, P. Psaras, and C. Nobili, J. Appl. Phys. **62**, 2290 (1987).
[19]S. P. Ashburn, M. C. Öztürk, G. Harris, and D. M. Maher, J. Appl. Phys. **74**, 4455 (1993).
[20]F. Wald and S. J. Michalik, J. Less-Common Met. **24**, 277 (1971).
[21]M. C. Ridgway, R. G. Elliman, R. Pascual, J. L. Whitton, and J.-M. Baribeau, Mater. Res. Soc. Symp. Proc. **311**, 155 (1993).
[22]C. Zaring, A. Pisch, J. Cardenas, P. Gas, and B. G. Svensson, J. Appl. Phys. **80**, 2742 (1996).
[23]C. Cytermann, E. Holzman, R. Brener, M. Fastow, M. Eizenberg, M. Glück, H. Kibbel, and U. König, J. Appl. Phys. **83**, 2019 (1998).
[24]L. P. Chen, C. T. Chou, G. W. Huang, and C. Y. Chang, Appl. Phys. Lett. **67**, 3001 (1995).
[25]P. L. Smith, C. M. Osburn, D. S. Wen, and G. McGuire, Mater. Res. Soc. Symp. Proc. **160**, 299 (1990).
[26]W. M. Chen, S. Pozder, Y. Limb, A. R. Sitaram, and B. Fiordalice, Mater. Res. Soc. Symp. Proc. **429**, 163 (1996).
[27]A. Eyal, R. Brener, R. Beserman, M. Eizenberg, Z. Atzmon, D. J. Smith, and J. W. Mayer, Appl. Phys. Lett. **69**, 64 (1996).
[28]Z. Wang, D. B. Aldrich, Y. L. Chen, D. E. Sayers, and R. J. Nemanich, Thin Solid Films **270**, 555 (1995).